THE JOURNAL OF PHYSICAL CHEMISTRY C
A JOURNAL OF THE AMERICAN CHEMICAL SOCIETY

pubs.acs.org/JPCC

Article

Interface- and Temperature-Sensitive Linear Electric Field Effects on Exciton Absorption of $CH_3NH_3PbI_3$ Perovskite Films

Published as part of The Journal of Physical Chemistry C virtual special issue "The Physical Chemistry of Perovskites".

Shailesh Rana, Kamlesh Awasthi, Eric Wei-Guang Diau, and Nobuhiro Ohta*

Cite This: *J. Phys. Chem. C* 2023, 127, 24383−24392

Read Online

ACCESS | Metrics & More | Article Recommendations | Supporting Information

ABSTRACT: The influence of applied electric field (F_A) on the absorption spectra of a methylammonium lead tri-iodide ($MAPbI_3$) crystalline film sandwiched between a fluorine-doped tin oxide (FTO) layer and a polymer film of poly(methyl methacrylate) (PMMA) (Sample I) and sandwiched between a compact layer of titanium oxide (cp-TiO_2) and a PMMA film (Sample II) has been investigated by first harmonic modulation spectroscopy on various temperatures in the range of 290−60 K. The linear electroabsorption spectra, EA(1*f*), of the $MAPbI_3$ film in Sample I showed very different behaviors in the temperature range above and below 200 K. EA(1*f*) spectra show a shape similar to the second derivative of the exciton absorption band having a Gaussian profile, and switching between positive and negative signs is generated at 290 K on alternating polarity of F_A. With decreasing temperature, the same tendency of F_A polarity-dependent EA(1*f*) switching was maintained until ∼200 K. At temperatures below 200 K, the inversion of the EA(1*f*) signal was found with the same field direction of F_A, and the signal intensity increased with decreasing temperature. In sample II, the polarity-dependent EA(1*f*) signal was negligibly small at room temperature but became prominent with decreasing temperature and followed the same trend as that in Sample I observed at temperatures below 200 K, indicating that the substrate on which the $MAPbI_3$ film was coated played a conclusive role as the origin of the polarity-dependent EA(1*f*) spectra. The second-derivative-like shape of the interface- and temperature-sensitive EA(1*f*) spectra is interpreted in terms of the polarity-dependent linear Stark shift of the exciton absorption band whose peak position depends on the temperature and substrate on which the $MAPbI_3$ film is coated.

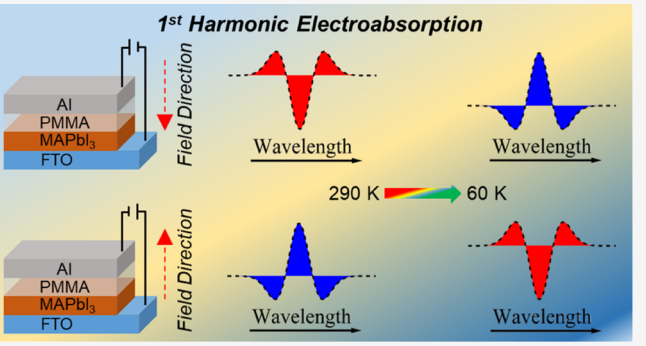

1. INTRODUCTION

In the past decade, state-of-the-art organic−inorganic halide perovskites (OIHPs) have emerged as a game-changer in optoelectronic applications.[1−4] Due to their superior optical and electrical properties, OIHPs have sparked the "perovskite-fever" that has inspired much research interest over the decade, boosting power conversion efficiency (PCE) from 3.8 to 25.5%.[1,5−9] Methylammonium lead tri-iodide ($MAPbI_3$) is one of the typical OIHPs that have attracted significant interest from the scientific community for fundamental and applied research.

Recently, electroabsorption (EA) spectroscopy, especially the quadratic effect of applied electric field on absorption spectra, has been used by monitoring the EA signal synchronized at the second harmonic of modulation frequency of the applied ac electric field (*M-F-AEF*). The resulting EA spectra, EA(2*f*), have gained popularity as a method to study the photophysics of exciton dissociation and charge generation and to determine the effective mass and exciton binding energy of OIHP films.[10−19] The Stark effect and the Franz−Keldysh (FK) oscillation have been used to interpret the measured EA(2*f*) signal. The kinetics of ion migration in the $MAPbI_3$ film has recently also been studied using EA(2*f*) measurements to examine how light intensity influences the shape and magnitude of the EA(2*f*) signals of exciton absorption with *M-F-AEF* between 40 Hz and 1 kHz.[20] In contrast with the EA(2*f*) spectra, linear electric field effects on absorption spectra, i.e., EA spectra obtained by monitoring the absorption signal synchronized at the first harmonic of *M-F-AEF*, EA(1*f*), have only been explored to a limited extent.[19,21] Linear electric field effects on absorption are usually expected for oriented

Received: August 19, 2023
Revised: November 20, 2023
Accepted: November 27, 2023
Published: December 8, 2023

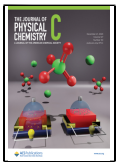

https://doi.org/10.1021/acs.jpcc.3c05603
J. Phys. Chem. C 2023, 127, 24383−24392

molecular systems or dye molecules aligned on the surface[22−24] to give the first-derivative shape of absorption spectra, coming from the linear Stark shift whose magnitude depends on the difference in electric dipole moment between the ground state and the photoexcited state. In randomly distributed systems, such a shift is very difficult to expect because of the cancellation of the signals coming from absorbers oriented in opposite directions although a linear electric field effect of band broadening and narrowing has been reported in some semiconductor quantum wells.[25−28]

Contrary to such general expectation of the linear Stark effect with a red shift or blue shift, we have observed EA(1*f*) spectra of the $MAPbI_3$ film, which are very similar in shape to the second derivative of the exciton absorption band at room temperature although the $MAPbI_3$ crystalline film may be regarded as a randomly distributed system. Such a shape is usually interpreted in terms of spectral broadening and narrowing, as explained in the analysis of the EA(2*f*) spectra.[29] It was also found that the EA(1*f*) spectra of the $MAPbI_3$ film sandwiched between the fluorine-doped tin oxide (FTO) layer and the polymer film of PMMA observed at room temperature are very different from the EA(1*f*) spectra of the $MAPbI_3$ film sandwiched between the compact layer of TiO_2 (cp-TiO_2) and the PMMA film, suggesting that the EA(1*f*) signal is very sensitive to the interface of the $MAPbI_3$ film. Switching of physical parameters such as absorbance is very important to design and develop novel materials of photonic and optoelectronic devices including switches and modulators.[30−33] Therefore, it is likely that the observed phenomena are applicable to photoswitching devices. At the moment, however, the mechanism of the interesting phenomena is not clear, and the elucidation of the mechanism will be important as fundamental research and for application.

$MAPbI_3$ crystalline films show a phase transition at ∼120 K from the tetragonal to the orthorhombic phase as the temperature of the film decreases. Therefore, it is also interesting to know whether EA(1*f*) depends on the crystal phase. In this work, the EA(1*f*) spectra of the $MAPbI_3$ film sandwiched between the FTO layer and the PMMA film were measured at temperatures in the range of 290−60 K, covering two different crystal phases of $MAPbI_3$ (tetragonal and orthorhombic). We also measured the EA(1*f*) intensity of the $MAPbI_3$ film sandwiched between the TiO_2 layer and the PMMA film as a function of wavelength. The measurements were done at various temperatures by inserting a cp-TiO_2 layer, as a layer between the FTO layer and the $MAPbI_3$ film. Based on the results, the following have been discussed: why the polarity-dependent EA(1*f*) spectra that are very similar in shape to the second derivative of the exciton absorption spectra are observed, why polarity dependence becomes reverse with decreasing temperature in some cases, and why the EA(1*f*) intensity depends on the substrate on which the $MAPbI_3$ film is coated.

When the $MAPbI_3$ film is used as a material for photovoltaic devices, the Fermi level position in the band gap as well as the efficiency of carrier doping may be tuned by the contacting material, and optimization of interfaces will be necessary for design and device optimization. In consideration of such problems, detailed information about the interfacial properties of materials on substrates is necessary. Even when the crystal morphology is similar, chemisorbed species, which is very different from the species inside the crystal, may be produced on the interface, and the present results show that such an interface specificity can be examined by the measurements of a linear electric field effect on absorption spectra.

2. EXPERIMENTAL SECTION

The samples of the $MAPbI_3$ crystalline film, which was sandwiched between the FTO layer and the PMMA film and sandwiched between the cp-TiO_2 layer and the PMMA film, were prepared with the same methods as the ones reported previously.[14,21] EA measurements were performed using the same methods as reported previously.[21,34] These have been described briefly.

2.1. Materials. Commercially available chemicals, i.e., titanium isopropoxide (TTIP) (97%, Aldrich), isopropyl alcohol (IPA) (99.5% anhydrous, Aldrich), chlorobenzene (CB) (99.8% anhydrous, Aldrich), dimethylformamide (DMF) (99.8%, Aldrich), methylammonium iodide (MAI, home-made), lead(II) iodide (PbI_2) (99.9%, TCI), PMMA (M_W ∼ 1,20,000, Aldrich), and toluene (spectrophotometry grade, J.T. Baker) were used without further purification. TiO_2 solution was prepared by adding TTIP (0.369 mL) into 2.53 mL of IPA. 2 M HCl (0.035 mL) solution in 2.53 mL of IPA was progressively added to the above-prepared TTIP solution with constant stirring at room temperature for 3 h.

$MAPbI_3$ precursor solution was prepared by mixing MAI and PbI_2 powders in a 1:1 molar ratio in DMF at 45 mass %. The mixture was stirred for 12 h in a nitrogen-purged glovebox at 70 °C.

2.2. Sample Preparation. The cp-TiO_2 layer was obtained by a spin-cast of the prepared TiO_2 solution on the top of the FTO-coated glass substrate at 4000 rpm for 30 s and kept on the hot plate at 100 °C for 10 min to remove the solvent. Then, the film was sintered at 450 °C for 1 h in the furnace. The FTO or TiO_2-coated FTO glass substrates were moved into a glovebox for the following deposition. A certain amount of the $MAPbI_3$ precursor solution was spin-coated on the top of FTO or cp-TiO_2-coated FTO substrates for 15 s at 5000 rpm to deposit the $MAPbI_3$ layer onto the substrates. Following 5 s of spinning, CB was dripped onto the center of the $MAPbI_3$ films as an antisolvent. A PMMA insulating film was coated on top of the $MAPbI_3$ film, which protects the prepared $MAPbI_3$ film from the outside environment and from direct contact with the metal electrode. Then, an aluminum (Al) layer, which had a thickness of ∼15 nm, was deposited via the vapor deposition method. Al and FTO layers were used as electrodes for the application of external electric fields, $\boldsymbol{F}_A$. The applied ac voltage was divided by the thickness of the sample to determine the strength of $\boldsymbol{F}_A$. Here, the $MAPbI_3$ film, which was sandwiched between the FTO layer and the PMMA film, is represented as Sample I, while the $MAPbI_3$ film, which was sandwiched between the cp-TiO_2 layer and the PMMA film, is represented as Sample II. The samples were prepared with the same method as the one reported in our previous paper.[21] The thickness of the TiO_2 film was estimated to be ∼60 nm by using the SEM image, and the thickness between the surface of the FTO layer and the surface of the PMMA film was estimated by using a profilometer (Veeco Dektak 150) to be ∼0.8 μm.

2.3. Optical Measurements. EA spectra, i.e., $\boldsymbol{F}_A$-induced change in absorption spectra, were obtained by monitoring the $\boldsymbol{F}_A$-induced change in the transmitted intensity of incident light (ΔI_{TLI}) with a JASCO FP-777 spectrometer, where a xenon (Xe) lamp was used as a light source. The light beam from the Xe lamp was irradiated on the sample in such a way that the

https://doi.org/10.1021/acs.jpcc.3c05603
J. Phys. Chem. C 2023, 127, 24383−24392

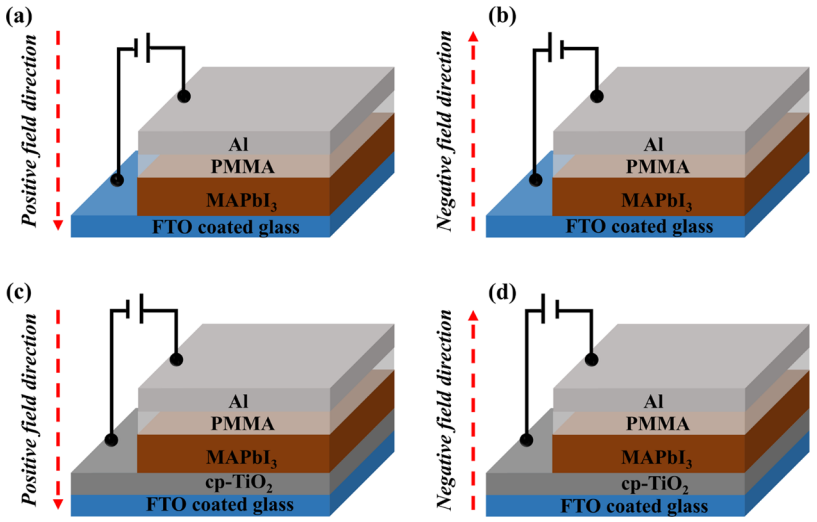

Figure 1. Schematic illustration of sample I (a, b) and sample II (c, d), where the $MAPbI_3$ film was sandwiched between the FTO layer and the PMMA film and sandwiched between the cp-TiO_2 layer and the PMMA film, respectively, and $\boldsymbol{F}_A$ with the positive direction (a, c) and negative direction (b, d).

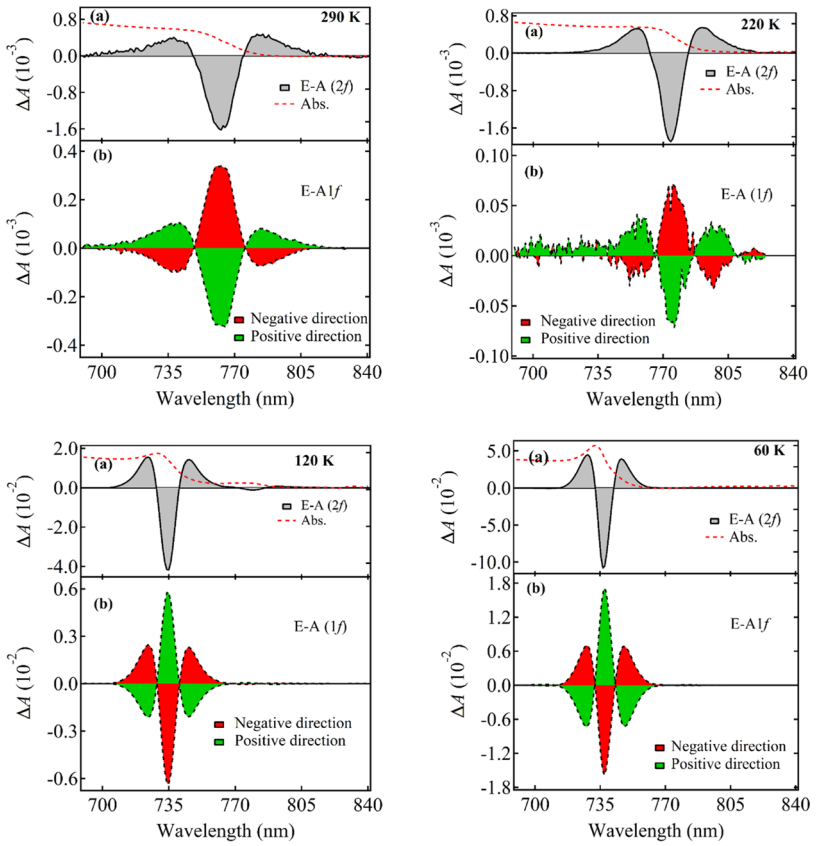

Figure 2. EA spectra of sample I at 290 K (upper left), 220 K (upper right), 120 K (lower left), and 60 K (lower right) observed with $\boldsymbol{F}_A$ having a strength of 0.3 MV cm^{-1} and modulation frequency of 1 kHz. EA(2*f*) spectra (**a**) and EA(1*f*) spectra (b) observed with the positive field direction (green) and negative field direction (red). See Figure 1 for the field direction. Absorption spectra are also shown by red dotted lines in (a).

light beam directly struck the sample side in a focus point. A fraction of the incident light was absorbed, and the resulting transmitted light intensity (I_{TLI}) was detected by an external photomultiplier tube (PMT). The signal from the PMT was amplified by using a preamplifier and divided into two channels. The dc component of I_{TLI} was recorded with a computer, and the ac component of ΔI_{TLI} synchronized with the modulated applied ac voltage was detected by a lock-in amplifier (SR830, SRS) at the first harmonic (1*f*) and second harmonic (2*f*) of *M-F-AEF*, i.e., 1 kHz. Then, EA intensity (ΔA) corresponding to 1*f* and 2*f* were obtained from $\Delta A = -\frac{1}{\log 10}\frac{\Delta I_{TLI}}{I_{TLI}}$ and $\Delta A = -\frac{2\sqrt{2}}{\log 10}\frac{\Delta I_{TLI}}{I_{TLI}}$, respectively.[21,35−38] A cryogenic refrigeration system (V202C5LR, Daikin) with quartz optical windows was used to record the temperature-sensitive EA spectra. A temperature controller (Model 9600,

https://doi.org/10.1021/acs.jpcc.3c05603
J. Phys. Chem. C 2023, 127, 24383−24392

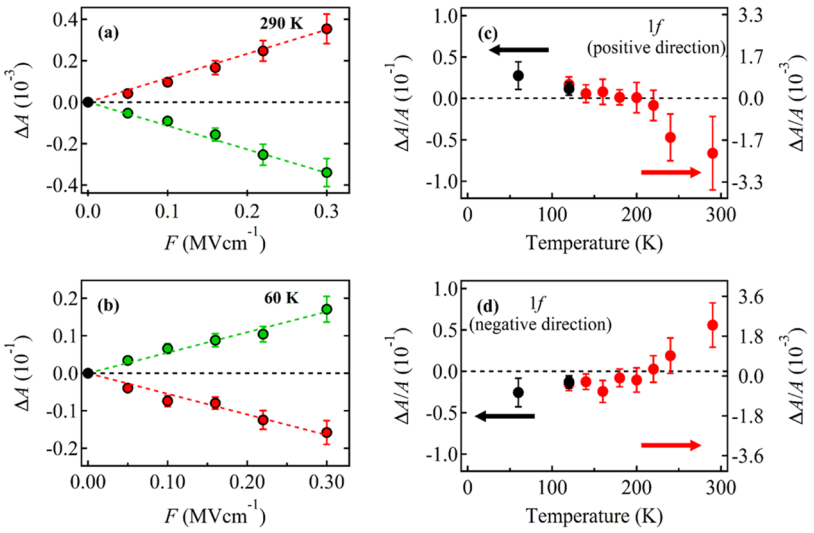

Figure 3. (Left) plots of the magnitudes of the EA(1*f*) signal in sample I obtained at the positive and negative peaks as a function of the strength of $\boldsymbol{F}_A$ at 290 K (a) and 60 K (b). EA(1*f*) signals obtained with positive and negative field directions are shown by green and red circles, respectively. (Right) plots of the intensity of the EA(1*f*) signal relative to the absorbance in sample I observed with $\boldsymbol{F}_A$ having a positive field direction (c) and negative field direction (d) as a function of temperature. The intensity was estimated with a field strength of 0.3 MV cm^{-1} at the peak of the EA(1*f*) spectra, which nearly corresponds to the peak of the exciton absorption band. Red and black circles in (c, d) show the data in tetragonal and orthorhombic phases, respectively.

Scientific Instruments) combined with a silicon diode thermometer (Si-410 A, Scientific Instruments) was used to control and monitor the substrate's temperature.

3. RESULTS AND DISCUSSION

A schematic illustration of Samples I and II, on which a sinusoidal ac field, $\boldsymbol{F}_A$, having 1 kHz (*M-F-AEF*) was applied, is shown in Figure 1. Positive and negative directions of $\boldsymbol{F}_A$ represent the directions from Al to FTO and FTO to Al, respectively. Unless otherwise noted, EA spectra were measured with a field strength of 0.3 MV cm^{-1} in each direction of $\boldsymbol{F}_A$, by monitoring ΔI_{TLI} synchronized at 1*f* of *M-F-AEF* of $\boldsymbol{F}_A$, and the observed spectra are represented as EA(1*f*) spectra. EA spectra were also measured by monitoring ΔI_{TLI} synchronized at 2*f* of *M-F-AEF* of $\boldsymbol{F}_A$ although the EA spectra observed at 2*f* at various temperatures and their analysis have already been reported.[14] Note that these E-A spectra are represented as EA(2*f*) spectra. It is noted that the *M-F-AEF* of $\boldsymbol{F}_A$ used in the present study, i.e., 1 kHz, is high enough to neglect the illumination power dependence.[20]

EA(1*f*) and EA(2*f*) spectra were measured at various temperatures in the range of 290−60 K. The results at 290, 220, 120, and 60 K are shown in Figure 2. The remaining results are shown in the Supporting Information (SI), i.e., Figure S1. It is found that the measured EA(1*f*) spectra remarkably depend on temperature, i.e., EA(1*f*) spectra are very sensitive to temperature. In every case, the EA(1*f*) intensity was linearly proportional to the strength of $\boldsymbol{F}_A$ up to 0.3 MV cm^{-1} (Figure 3), while the EA(2*f*) intensity was proportional to the square of the strength of $\boldsymbol{F}_A$, as already reported.[12,14] The EA(2*f*) spectra obtained at various temperatures were essentially the same as the ones already reported.[14,15] The EA(2*f*) spectra could be interpreted in terms of the quadratic Stark effect, and the EA(2*f*) spectra could be reproduced by a linear combination of the zeroth, first, and second derivatives of the exciton absorption band, which gives a Gaussian shape. Since the largest contribution is the second-derivative component, the spectral shape of the EA(2*f*) spectra mainly corresponds to the spectral broadening of the exciton absorption band, which results from the change in the electric dipole moment following photoexcitation, i.e., $\Delta\mu$. From the contribution of the first-derivative component, the magnitude of the change in polarizability following excitation into the exciton band, i.e., $\Delta\alpha$, was also determined, and the magnitudes of $\Delta\mu$ and $\Delta\alpha$ at different temperatures have been reported in our previous paper.[14] Temperature-dependent EA(1*f*) spectra, which also depend on the polarity of $\boldsymbol{F}_A$, are very different from the EA(2*f*) spectra.

The EA(1*f*) spectra of Sample I observed with positive and negative directions of $\boldsymbol{F}_A$ are essentially the same in shape but opposite in positive and negative signs at any temperature. Regardless of the amplitude and sign of the EA(1*f*) signal, the shape and peak position of the EA(1*f*) spectra are comparable to the ones of the EA(2*f*) spectra in most cases. The polarity dependence in the EA(1*f*) spectra has also been found to depend on temperature in Sample I. The EA(1*f*) spectra observed at 290 K are essentially the same as those we reported earlier;[21] a shape similar to the positive or negative second derivative of the exciton absorption band was observed with a positive or negative direction of $\boldsymbol{F}_A$, respectively (see Figure 2). As shown in Figures 2 and S1 of the SI, the same is true at 240 and 220 K although the signal intensity of EA(1*f*) became weaker with decreasing temperature. As the temperature further decreased, an inversion of the polarity dependence was observed; positive and negative second-derivative shapes were observed with negative and positive directions of $\boldsymbol{F}_A$, respectively, and not with positive and negative directions. In the result, EA(1*f*) spectra at 120 and 60 K are completely inverted, in comparison with the ones at 290−220 K (see Figure 2). The temperature dependence of the peak intensity of the EA(1*f*) spectra observed with the positive or negative direction of $\boldsymbol{F}_A$ is shown in Figure 3, which clearly indicates the inversion of the polarity dependence with decreasing temperature. It is known that the phase transition occurs at around 120 K from the tetragonal to the orthorhombic phase in the $MAPbI_3$ crystalline film as the temperature decreases from

https://doi.org/10.1021/acs.jpcc.3c05603
J. Phys. Chem. C 2023, 127, 24383−24392

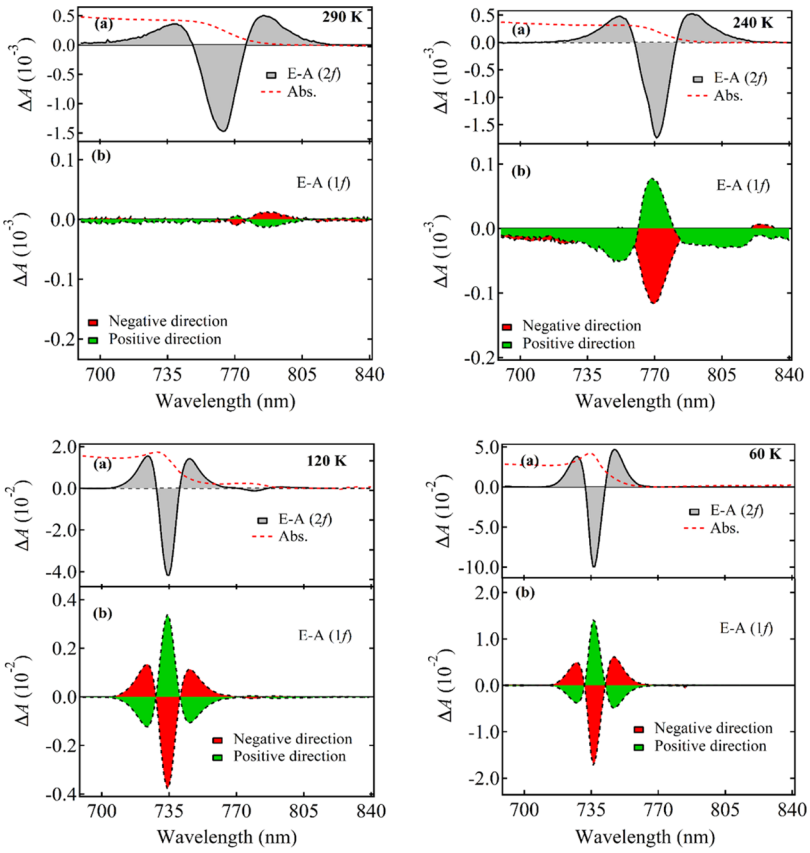

Figure 4. EA spectra of sample II at 290 K (upper left), 240 K (upper right), 120 K (lower left), and 60 K (lower right) obtained with $\boldsymbol{F}_A$ having a strength of 0.3 MV cm^{-1} and a modulation frequency of 1 kHz. EA(2*f*) spectra (a) and EA(1*f*) spectra (b) obtained with the positive field direction (green) and the negative field direction (red). See Figure 1 for the field direction. Absorption spectra are also shown by the red dotted lines in (a).

room temperature.[14,39,40] In fact, the position that had the minimum intensity in the EA(2*f*) spectra suddenly changed with decreasing temperature from 140 to 120 K, as shown in Figure S2 of the SI. As shown in Figures 2 and S1 of the SI, the inversion of the polarity dependence of EA(1*f*) observed with decreasing temperature did not follow the phase transition, and the inversion occurred at around 160 K, where the $MAPbI_3$ crystal is expected to be still in the tetragonal phase.

When the direction of the applied electric field was reversed, the change in absorption intensity, i.e., the change in transmitted light intensity, became opposite. A similar reversal in absorption intensity could also be observed in Sample I by changing the temperature, cf., the results at 290 and 60 K in Figure 2. Then, there is a strong possibility that this kind of reversibility between the increase and decrease of transmitted light intensity by changing the direction of $\boldsymbol{F}_A$ and by changing the temperature can be used as a photoswitching device.

In contrast with Sample I, the EA(1*f*) signal of Sample II was extremely weak at room temperature.[21] Then, the temperature dependence of EA(1*f*) and EA(2*f*) spectra of Sample II was examined; the EA spectra of Sample II were also measured at various temperatures ranging from 290 to 60 K. The results at 290, 240, 120, and 60 K are shown in Figure 4. The remaining results are shown in Figure S3 of the SI. The EA(2*f*) spectra of Sample II are nearly the same as the ones observed in Sample I, as shown in Figure S2 of the SI. Prominent EA(1*f*) spectra were observed in Sample II at all temperatures except at 290 K, where the signal was not extremely weak, and EA(1*f*) spectra showed a similar polarity dependence at every temperature ranging from 240 to 60 K; EA(1*f*) spectra having a second-derivative-like shape of the Gaussian profile were observed at temperatures below 240 K, and the magnitude of the EA(1*f*) signal increased as the temperature decreased. On alternating the polarity of $\boldsymbol{F}_A$, the inversion of EA(1*f*) spectra was observed, as in the case of Sample I; EA(1*f*) spectra in Sample II showed a shape similar to the positive or negative second derivative of a Gaussian profile, with a negative or positive direction of $\boldsymbol{F}_A$, respectively. Note that the EA(1*f*) spectra of Sample II are opposite in positive and negative signs to the ones of Sample I observed at temperatures above 220 K (cf. Figures 2 and 4). It was also confirmed that the magnitude of the EA(1*f*) intensity in Sample II linearly increased on increasing the applied field strength (Figure S4 of the SI), as in the case of Sample I, indicating that the observed EA(1*f*) spectra in Sample II also originated from the linear electric field effect. The magnitude of the EA(1*f*) signal of Sample II suddenly increased as the temperature decreased from 290 to 240 K and then gradually changed on further decreasing the temperature, as shown in Figure 5. It was also confirmed that the magnitude of the EA(1*f*) signal in the orthorhombic phase was much larger than that in the tetragonal phase in both Samples I and II.

In the quadratic Stark effect, where ΔA is proportional to the square of the strength of $\boldsymbol{F}_A$, spectral shift and broadening characterized by the first and second derivatives of the absorption spectra are expected to arise from $\Delta\alpha$ and $\Delta\mu$, respectively.[14] The values of $\Delta\alpha$ and $\Delta\mu$ determined from the EA(2*f*) spectra can be regarded as the material parameters, but

https://doi.org/10.1021/acs.jpcc.3c05603
J. Phys. Chem. C 2023, 127, 24383−24392

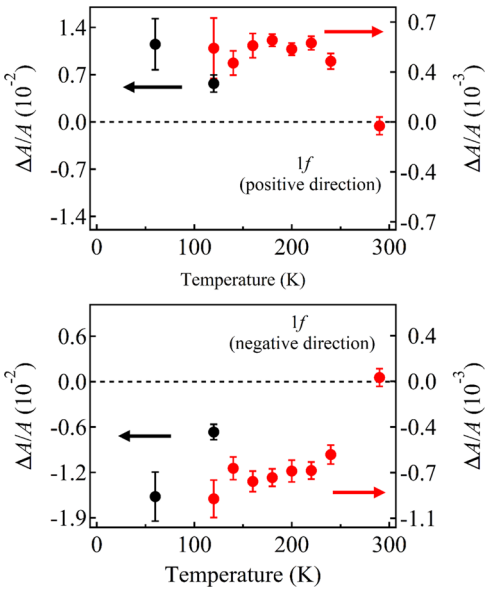

Figure 5. Plots of the intensity of the EA(1*f*) signal relative to absorbance in sample II observed with F_A having a positive field direction (upper) and a negative field direction (lower) as a function of temperature. The strength of F_A was 0.3 MV cm^{-1}. The intensity was estimated at the peak of the EA(1*f*) spectra. The red and black circles show the data at tetragonal and orthorhombic phases, respectively.

information about the interface of the sample is not included. As a linear electric field effect on absorption spectra, the spectral shift resulting from $\Delta\mu$, i.e., $-\Delta\mu F_A$, can be considered. If materials are randomly distributed in space, this effect is canceled out with dipoles that have opposite directions from each other. Only for the oriented system the linear E-A spectra, which show a similar shape to the first derivative of the absorption spectrum, are expected. Contrary to the expectation, the observed EA(1*f*) spectra are very similar in shape to the second derivative of a Gaussian profile, implying spectral broadening and narrowing on alternating polarity of F_A. In fact, the shape of the EA(1*f*) spectra can be roughly reproduced by assuming broadening or narrowing of the exciton absorption band, whose bandwidth was estimated at each temperature by analyzing the EA(2*f*) spectra.[14] As shown in Figure S5 of the SI, for instance, the EA(1*f*) spectra of Sample I are roughly reproduced by assuming broadening or narrowing of the exciton band by ∼0.8−1.0 at 290 K and by 1.0−3.0 cm^{-1} at 60 K, respectively, depending on the polarity of F_A. Note that the exciton absorption band was determined to have a Gaussian profile with a full width at half-maximum (fwhm) of 535 cm^{-1} at 290 K and 245 cm^{-1} at 60 K.[14] Even if the shape of the EA(1*f*) spectra can be reproduced, a simple concept of field-induced spectral broadening and narrowing of the exciton absorption band seems to be inappropriate as the origin of the present EA(1*f*) spectra caused by the linear electric field effect.

The linear Stark effect gives a spectral shift caused by $\Delta\mu$. Inside $MAPbI_3$ films, where the direction of $\Delta\mu$ is considered to be randomly oriented, the spectral shift can be canceled as an overall average, resulting in no signal of the EA(1f), as already mentioned. In Samples I and II, however, things may be different. Molecular alignment at both interfaces may be regarded as opposite to each other, i.e., the direction of $\Delta\mu$ of materials that are located on both interfaces may be considered to be opposite to each other. In such a case, the spectral shift induced by F_A contributed from $MAPbI_3$ located at both interfaces may be canceled if the absorption bands of the $MAPbI_3$ film contacted on the FTO or cp-TiO_2 layer and the PMMA film are the same. If the position of the exciton absorption band is not the same at both interfaces, however, the EA(1*f*) signal may be observable. The exciton bands of Sample I at the interface on the FTO layer and at the other interlayer on the PMMA film may give the opposite shift to each other in the presence of F_A because of the opposite direction of the electric dipole moment, $\boldsymbol{\mu}$, of $MAPbI_3$ on both interfaces. Then, a shape similar to the second derivative of a Gaussian profile may be reproduced for the EA(1*f*) spectra, as shown in Figure 6, depending on the difference in the position of the exciton absorption bands at both interfaces. Note that the first derivative of absorbance, i.e., $dA/d\nu$, is also shown in Figure 6. Note that a small field-induced change in absorbance, i.e., ΔA, is given by $(dA/d\nu)(-\Delta\boldsymbol{\mu}F_A)$ and that the magnitude of $\Delta\mu$ of the $MAPbI_3$ film estimated from the EA(2*f*) spectra

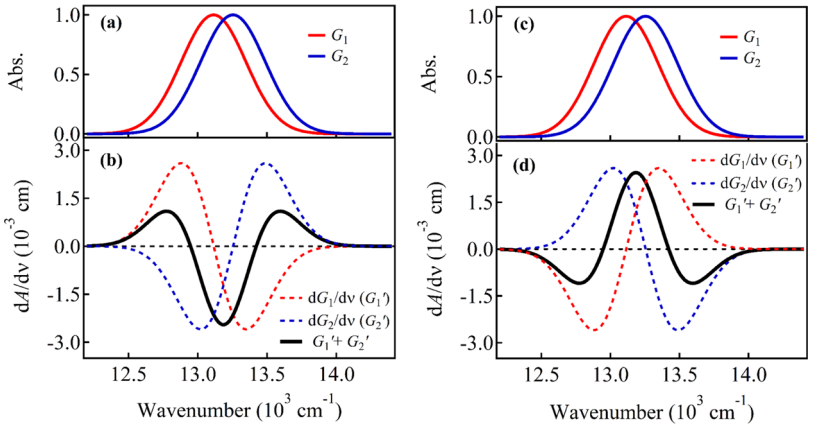

Figure 6. EA(1*f*) spectra resulting from two absorption bands that have different peak positions and show opposite Stark shift to each other at different interfaces. It is assumed that the absorption spectra G_1 (red) and G_2 (blue) show red and blue shifts in the presence of F_A, respectively, (a, b) and that G_1 (red) and G_2 (blue) show blue and red shifts, respectively (c, d). These changes correspond to switching of the direction of F_A. The spectral shift is given by the first derivative of the absorption spectra, i.e., $dG_1/d\nu$ (G_1') and $dG_2/d\nu$ (G_2'), and the EA(1*f*) spectrum is given by $G_1' + G_2'$.

https://doi.org/10.1021/acs.jpcc.3c05603
J. Phys. Chem. C 2023, 127, 24383−24392

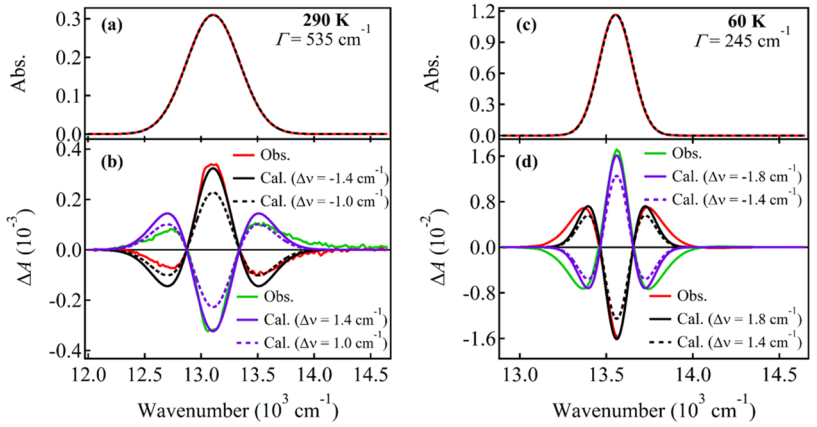

Figure 7. Simulation of the EA(1*f*) spectra of sample I at 290 K (left) and 60 K (right) with a Gaussian profile of the absorption spectra having fwhm values of 535 cm^{-1} (a) and 245 cm^{-1} (c). EA(1*f*) spectra are simulated with $\Delta\nu$ = 1.0 and 1.4 cm^{-1} (b) and −1.4 and −1.8 cm^{-1} (d) with a positive direction of $\boldsymbol{F}_A$. EA(1*f*) spectra are also simulated with $\Delta\nu$ = −1.0 and −1.4 cm^{-1} (b) and 1.4 and 1.8 cm^{-1} (d) with a negative direction of $\boldsymbol{F}_A$. Red and green lines show the observed spectra, and black and violet lines show the simulated spectra. See Figure 8 for the positive and negative values of $\Delta\nu$, which is the energy separation between two absorption peaks in the absence of $\boldsymbol{F}_A$.

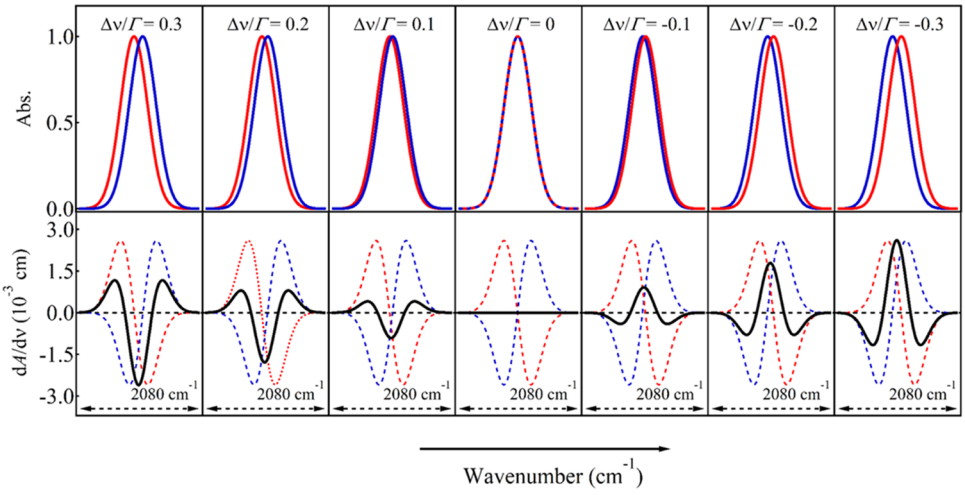

Figure 8. EA(1*f*) spectra depend on the energy separation ($\Delta\nu$) between peaks of two absorption bands at ν_1 and ν_2, i.e., $\Delta\nu = \nu_2 - \nu_1$. Absorption spectra given by red and blue lines are assumed to show red shift and blue shift, respectively, in the presence of $\boldsymbol{F}_A$, and the first derivatives of these absorption bands are shown below. EA(1*f*) spectra given by the solid line in the lower figures come from two absorption bands having different peaks and opposite Stark shift to each other, i.e., black lines in the lower figures show the sum of the first derivatives of these two absorption bands.

was reported in the SI of our previous paper.[14] At 290, 220, 120, and 60 K, for example, the magnitudes of $\Delta\mu$ are ∼8, ∼6, ∼12, and ∼14 D, respectively, resulting in the magnitudes of $\boldsymbol{\Delta\mu F}_A$ of ∼40, ∼30, ∼60, and ∼70 cm^{-1} with 0.3 MV cm^{-1} for $\boldsymbol{F}_A$. With this scheme, the polarity dependence of the EA(1*f*) spectra can be interpreted well because positive and negative signs of the EA spectra of $MAPbI_3$ at both interfaces are reversed by changing the direction of $\boldsymbol{F}_A$. As shown in Figure 7, the EA(1*f*) spectra observed at 290 and 60 K in Sample I can be reproduced quite well by considering a difference between peak positions ($\Delta\nu$) in the absence of $\boldsymbol{F}_A$ by 1.0−1.4 and 1.4−1.8 cm^{-1}, respectively, for exciton absorption bands of $MAPbI_3$ at different interfaces. The fwhm (Γ) values of the exciton absorption band are assumed to be 535 and 245 cm^{-1}, respectively, at 290 and 60 K.[14] The results that both observed and simulated EA(1*f*) spectra are not completely consistent may be due to the simple assumption that the exciton absorption band shows a Gaussian profile.

The inversion of the polarity-dependent E-A spectra with decreasing temperature in Sample I can also be explained by assuming a change in the positional relationship between the exciton absorption bands of $MAPbI_3$ at different interfaces, as shown in Figure 8, where the sum of ΔA, i.e., the sum of $dA/d\nu$ at both interfaces, is given as a function of the energy difference between peak positions of the bands of $MAPbI_3$ located at different interfaces. The exciton absorption band of $MAPbI_3$ on the FTO layer may be located in the higher wavenumber region than that on the PMMA film at room temperature, whereas the exciton absorption band of $MAPbI_3$ on the FTO layer may be located in the lower wavenumber region than that on the PMMA film at temperatures below 200 K. As the energy separation between absorption bands of $MAPbI_3$ located at different interfaces becomes smaller, the magnitude of the EA(1*f*) signal becomes smaller, as shown in Figure 8. The fact that the EA(1*f*) signal in Sample I became smaller and finally the positive and negative signs of the spectra became opposite with decreasing temperature from 290 to 60 K indicates that energy separation between exciton absorption bands of the $MAPbI_3$ film located at different interfaces became smaller with decreasing temperature and finally the

https://doi.org/10.1021/acs.jpcc.3c05603
J. Phys. Chem. C 2023, 127, 24383−24392

positional relationship between the absorption bands reversed, as shown in Figure 8.

It is well-known that the peak of the exciton absorption band of the $MAPbI_3$ film depends on temperature remarkably,[14] and the absorption peak is expected to be different at each temperature between $MAPbI_3$ films on the FTO layer and on the PMMA film. Further, the electronic structure of the $MAPbI_3$ film has been reported to depend on the substrate on which the $MAPbI_3$ film is coated, including the possibility of a chemical reaction at the interface.[41,42] The present results of EA(1f) spectra imply that the morphology of $MAPbI_3$ at the interface significantly depends on the contacted substrate and on temperature, even when the morphology of the bulk crystal is independent of the substrate on which the $MAPbI_3$ film is coated. In a recent paper,[43] the importance of interlayer morphology in perovskite crystallization has been emphasized in relation to photovoltaic performance and $I-V$ hysteresis in perovskite solar cells.

The temperature dependence of the EA(1f) spectra of Sample II can also be interpreted in terms of the above-mentioned model. The result that the EA(1f) signal is very weak at room temperature suggests that the peak position of the exciton absorption band of Sample II is nearly the same at both interfaces at room temperature. As the temperature decreased, the difference in peak position between the absorption bands of $MAPbI_3$ located at both interfaces is considered to become larger. In contrast with Sample I, probably there is no change in the positional relationship between exciton absorption bands of $MAPbI_3$ at both interfaces, even with decreasing temperature; in Sample II, the absorption peak of $MAPbI_3$ located on the cp-TiO_2 layer may be located in the longer wavelength than that of $MAPbI_3$ on the PMMA film (or vice versa) at temperatures in the range of 290−60 K, and the difference between absorption peaks is considered to become larger with decreasing temperature.

The present results clearly show that the interface of the $MAPbI_3$ nanocrystalline film on substrates is extremely important for the EA(1f) spectra. In quantum well (QW) excitons, it was suggested that interface roughness might show a linear correlation with the field contribution to the line width of the exciton,[25] resulting in switching between broadening and narrowing of the bandwidth of the exciton absorption band with a change in field polarity. The present results seem to be very similar to the above-mentioned phenomena expected in QW although the present sample of the $MAPbI_3$ film was just sandwiched with different substrates. In both cases, there is no doubt that the interface of the film plays a conclusive role in the appearance of the linear electric field effect, which reminds us of narrowing and broadening of the spectral bandwidth, depending on the polarity of $\boldsymbol{F}_A$. There is no doubt that EA(1f) signals are strongly related to the electronic structure of materials on the interface, and selection of the substrate on which materials are coated is extremely important to consider for optoelectronic devices such as photovoltaic cells. The present results show that interfacial properties of perovskite materials are very sensitive not only to the substrate but also to temperature, implying that device performance also shows a sensitive temperature dependence. At the moment, however, the relation between the EA(1f) signal and device performance in optoelectronic devices is not known well, which will be a future problem.

Besides the concept that the linear Stark shift which gives different behaviors at both interfaces plays a conclusive role in the appearance of the EA(1f) signal, it may also be necessary to consider the possibility that the spectral bandwidth itself changes with applied electric fields as the origin of the EA(1f) spectra observed in the present study. A temperature-sensitive exciton bandwidth in a semiconductor at temperature T, $\Gamma_{EP}(T)$, is related to an exciton−phonon interaction and given by $\Gamma_0 + \gamma T + \gamma_B N_L(T)$,[44] where the first term corresponds to temperature-independent broadening, caused by scattering due to impurities and/or imperfections. The second and third terms are caused by interactions of the exciton with acoustic phonons and LO phonons, respectively. γ and γ_B are the coupling strengths between the exciton and acoustic phonon and between the exciton and LO phonon, respectively; $N_L(T)$ is given by $1/[\exp(E_L/k_BT) - 1]$, with phonon energy E_L and Boltzmann constant k_B. LO phonons might scatter excitons to bound and continuum states. The value of $\Gamma_{EP}(T)$ of the $MAPbI_3$ film, i.e., fwhm, was evaluated by the analysis of the EA(2f) spectra,[14] and it was shown that $\Gamma_{EP}(T)$ monotonically decreased as a function of T^{-1}. However, it is unlikely that $\Gamma_{EP}(T)$ shows a polarity-dependent linear field effect. Therefore, the linear Stark shift which depends on the interface is the most probable as a mechanism to interpret the EA(1f) signal observed for the $MAPbI_3$ films.

4. CONCLUSIONS

Temperature-sensitive EA(1f) spectra depend on the substrate on which the $MAPbI_3$ film was coated; EA(1f) spectra of $MAPbI_3$ films sandwiched between the FTO layer and the PMMA film (Sample I) and between the cp-TiO_2 layer and the PMMA film (Sample II) show very different temperature dependences from each other, indicating that EA(1f) spectra depend on the temperature and substrate on which the $MAPbI_3$ film is coated. In both Samples I and II, EA(1f) spectra, which are similar in shape to the second derivative of the exciton absorption band having a Gaussian profile, depend on polarity of $\boldsymbol{F}_A$; on alternating the polarity of $\boldsymbol{F}_A$, switching between positive and negative second-derivative like shapes was found in the EA(1f) spectra at any temperature. The signal intensity of EA(1f) in Sample I decreased on decreasing the temperature from room temperature, and the inversion of the polarity dependence was observed at temperatures below 200 K. After the inversion, the magnitude of the signal intensity of EA(1f) increased with a further decrease in temperature, especially in the orthorhombic phase. In Sample II, the EA(1f) signal, which was extremely weak at 290 K, increased with decreasing temperature with the same polarity dependence as the one observed in Sample I at temperatures below 200 K. The clear difference in the EA(1f) spectra between Samples I and II indicates that the interface between the $MAPbI_3$ film and the substrate on which the $MAPbI_3$ film is coated plays a crucial role in the EA(1f) spectra of the exciton absorption band of $MAPbI_3$ films. The shape similar to the second derivative of a Gaussian profile is interpreted in terms of the linear Stark shift of the exciton absorption band of the $MAPbI_3$ film by assuming that the absorption peak of the exciton band of the $MAPbI_3$ film is different at both interfaces. Temperature-dependent inversion of the polarity-dependent EA(1f) spectra in Sample I is interpreted in terms of reversal of the positional relationship between exciton absorption bands of $MAPbI_3$ at both interfaces. In the results, the switching of the EA(1f) spectra can be observed by alternating the polarity of $\boldsymbol{F}_A$ in Samples I and II and also by changing the temperature in Sample I.

https://doi.org/10.1021/acs.jpcc.3c05603
J. Phys. Chem. C 2023, 127, 24383−24392

■ ASSOCIATED CONTENT

Supporting Information

The Supporting Information is available free of charge at https://pubs.acs.org/doi/10.1021/acs.jpcc.3c05603.

E-A spectra of Sample I at 240, 200, 180, 160, and 140 K; EA(2*f*) spectra of Samples I and II at different temperatures; EA spectra of Sample II at 220, 200, 180, 160, and 140 K; electric field strength dependence of EA(1*f*) intensity of Sample II, and simulation of EA(1*f*) spectra by considering spectral broadening and narrowing (PDF)

■ AUTHOR INFORMATION

Corresponding Author

Nobuhiro Ohta − *Department of Applied Chemistry and Institute of Molecular Science, National Yang Ming Chiao Tung University, Hsinchu 300093, Taiwan; Center for Emergent Functional Matter Science, National Yang Ming Chiao Tung University, Hsinchu 300093, Taiwan;* orcid.org/0000-0003-4255-6448; Email: nohta@nycu.edu.tw

Authors

Shailesh Rana − *Department of Applied Chemistry and Institute of Molecular Science, National Yang Ming Chiao Tung University, Hsinchu 300093, Taiwan;* orcid.org/0000-0002-4349-101X

Kamlesh Awasthi − *Department of Applied Chemistry and Institute of Molecular Science, National Yang Ming Chiao Tung University, Hsinchu 300093, Taiwan; Center for Emergent Functional Matter Science, National Yang Ming Chiao Tung University, Hsinchu 300093, Taiwan;* orcid.org/0000-0001-7852-059X

Eric Wei-Guang Diau − *Department of Applied Chemistry and Institute of Molecular Science, National Yang Ming Chiao Tung University, Hsinchu 300093, Taiwan; Center for Emergent Functional Matter Science, National Yang Ming Chiao Tung University, Hsinchu 300093, Taiwan;* orcid.org/0000-0001-6113-5679

Complete contact information is available at: https://pubs.acs.org/10.1021/acs.jpcc.3c05603

Notes

The authors declare no competing financial interest.

■ ACKNOWLEDGMENTS

This work was supported by the National Science and Technology Council in Taiwan (MOST111-2634-F-A49-007 and MOST111-2113-M-A49-015). This work was also supported by the Center for Emergent Functional Matter Science of National Yang Ming Chiao Tung University from The Featured Areas Research Center Program within the framework of the Higher Education Sprout Project by the Ministry of Education in Taiwan.

■ REFERENCES

(1) Kojima, A.; Teshima, K.; Shirai, Y.; Miyasaka, T. Organometal Halide Perovskites as Visible-Light Sensitizers for Photovoltaic Cells. *J. Am. Chem. Soc.* **2009**, *131*, 6050−6051.

(2) Pammi, S. V. N.; Tran, V. D.; Maddaka, R.; Eom, J. H.; Jung, J. S.; Jeong, H. M.; Kim, M. D.; Pecunia, V.; Yoon, S. G. Bromine Doping of $MAPbI_3$ Films Deposited Via Chemical Vapor Deposition Enables Efficient and Photo-Stable Self-Powered Photodetectors. *Adv. Opt. Mater.* **2020**, *8*, No. 2000845.

(3) Zhao, L.; Lee, K. M.; Roh, K.; Khan, S. U. Z.; Rand, B. P. Improved Outcoupling Efficiency and Stability of Perovskite Light-Emitting Diodes Using Thin Emitting Layers. *Adv. Mater.* **2019**, *31*, No. 1805836.

(4) Gu, C.; Lee, J. S. Flexible Hybrid Organic-Inorganic Perovskite Memory. *ACS Nano* **2016**, *10*, 5413−5418.

(5) Lee, M. M.; Teuscher, J.; Miyasaka, T.; Murakami, T. N.; Snaith, H. J. Efficient Hybrid Solar Cells Based on Meso-Superstructured Organometal Halide Perovskites. *Science* **2012**, *338*, 643−647.

(6) Burschka, J.; Pellet, N.; Moon, S. J.; Humphry-Baker, R.; Gao, P.; Nazeeruddin, M. K.; Grätzel, M. Sequential Deposition as a Route to High-Performance Perovskite-Sensitized Solar Cells. *Nature* **2013**, *499*, 316−319.

(7) Liu, M.; Johnston, M. B.; Snaith, H. J. Efficient Planar Heterojunction Perovskite Solar Cells by Vapor Deposition. *Nature* **2013**, *501*, 395−398.

(8) Heo, J. H.; Im, S. H.; Noh, J. H.; Mandal, T. N.; Lim, C. S.; Chang, J. A.; Lee, Y. H.; Kim, H. J.; Sarkar, A.; Nazeeruddin, M. K.; Grätzel, M.; Seok, S., II. Efficient Inorganic-Organic Hybrid Heterojunction Solar Cells Containing Perovskite Compound and Polymeric Hole Conductors. *Nat. Photonics* **2013**, *7*, 486−491.

(9) Min, H.; Lee, D. Y.; Kim, J.; Kim, G.; Lee, K. S.; Kim, J.; Paik, M. J.; Kim, Y. K.; Kim, K. S.; Kim, M. G.; Shin, T. J.; Seok, S., II. Perovskite Solar Cells with Atomically Coherent Interlayers on SnO_2 Electrodes. *Nature* **2021**, *598*, 444−450.

(10) Wu, X.; Yu, H.; Li, L.; Li, L.; Wang, F.; Xu, H.; Zhao, N. Composition-Dependent Light-Induced Dipole Moment Change in Organometal Halide Perovskites. *J. Phys. Chem. C* **2015**, *119*, 1253−1259.

(11) Ziffer, M. E.; Mohammed, J. C.; Ginger, D. S. Electroabsorption Spectroscopy Measurements of the Exciton Binding Energy, Electron-Hole Reduced Effective Mass, and Band Gap in the Perovskite $CH_3NH_3PbI_3$. *ACS Photonics* **2016**, *3*, 1060−1068.

(12) Awasthi, K.; Du, K. B.; Wang, C. Y.; Tsai, C. L.; Hamada, M.; Narra, S.; Diau, E. W. G.; Ohta, N. Electroabsorption Studies of Multicolored Lead Halide Perovskite Nanocrystalline Solid Films. *ACS Photonics* **2018**, *5*, 2408−2417.

(13) Ruf, F.; Magin, A.; Schultes, M.; Ahlswede, E.; Kalt, H.; Hetterich, M. Excitonic Nature of Optical Transitions in Electroabsorption Spectra of Perovskite Solar Cells. *Appl. Phys. Lett.* **2018**, *112*, No. 083902.

(14) Hamada, M.; Rana, S.; Jokar, E.; Awasthi, K.; Diau, E. W. G.; Ohta, N. Temperature-Dependent Electroabsorption Spectra and Exciton Binding Energy in a Perovskite $CH_3NH_3PbI_3$ Nanocrystalline Film. *ACS Appl. Energy Mater.* **2020**, *3*, 11830−11840.

(15) Leijtens, T.; Kandada, A. R. S.; Eperon, G. E.; Grancini, G.; D'Innocenzo, V.; Ball, J. M.; Stranks, S. D.; Snaith, H. J.; Petrozza, A. Modulating the Electron−Hole Interaction in a Hybrid Lead Halide Perovskite with an Electric Field. *J. Am. Chem. Soc.* **2015**, *137*, 15451−15459.

(16) Amerling, E.; Baniya, S.; Lafalce, E.; Zhang, C.; Vardeny, Z. V.; Whittaker-Brooks, L. Electroabsorption Spectroscopy Studies of $(C_4H_9NH_3)_2PbI_4$ Organic−Inorganic Hybrid Perovskite Multiple Quantum Wells. *J. Phys. Chem. Lett.* **2017**, *8*, 4557−4564.

(17) Kattoor, V.; Awasthi, K.; Jokar, E.; Diau, E. W. G.; Ohta, N. Integral Method Analysis of Electroabsorption Spectra and Electrophotoluminescence Study of $(C_4H_9NH_3)_2PbI_4$ Organic−Inorganic Quantum Well. *J. Phys. Chem. C* **2018**, *122*, 26623−26634.

(18) Kattoor, V.; Awasthi, K.; Jokar, E.; Diau, E. W. G.; Ohta, N. Enhanced Dissociation of Hot Excitons with an Applied Electric Field under Low-Power Photoexcitation in Two-Dimensional Perovskite Quantum Wells. *J. Phys. Chem. Lett.* **2019**, *10*, 4752−4757.

(19) Roiati, V.; Mosconi, E.; Listorti, A.; Colella, S.; Gigli, G.; De Angelis, F. Stark Effect in Perovskite/TiO_2 Solar Cells: Evidence of Local Interfacial Order. *Nano Lett.* **2014**, *14*, 2168−2174.

(20) Rana, S.; Awasthi, K.; Diau, E. W. G.; Ohta, N. Illumination Power-Dependent Electroabsorption of Excitons in a $CH_3NH_3PbI_3$ Perovskite Film. *J. Phys. Chem. C* **2021**, *125*, 27631−27637.
(21) Awasthi, K.; Kala, K.; Rana, S.; Diau, E. W. G.; Ohta, N. Switching between Spectral Broadening and Narrowing of the Exciton Absorption Band of a $CH_3NH_3PbI_3$ Film on Altering the Polarity of an Applied Electric Field. *Appl. Phys. Lett.* **2020**, *116*, No. 251101.
(22) Bücher, H.; Kuhn, H. Difference between Ground and Excited State Dipole Moments and Polarizabilities as Determined from Electrochromism of Scheibe-Dye-aggregates in Monolayer Assemblies. *Z. Naturforsch. B* **1970**, *25*, 1323−1327.
(23) Ohta, N.; Okazaki, S.; Yamazaki, I. Stark Shift in Absorption Spectra of Langmuir-Blodgett Mixed Monolayer Films: New Finding of a Complex Formation of Chromophoric Oxacyanine. *Chem. Phys. Lett.* **1994**, *229*, 394−400.
(24) Cappel, U. B.; Feldt, S. M.; Schöneboom, J.; Hagfeldt, A.; Boschloo, G. The Influence of Local Electric Fields on Photoinduced Absorption in Dye-Sensitized Solar Cells. *J. Am. Chem. Soc.* **2010**, *132*, 9096−9101.
(25) Ponomarev, I. V.; Deych, L. I.; Lisyansky, A. A. Electric-Field-Induced Narrowing of Exciton Linewidth. *Phys. Rev. B* **2005**, *72*, No. 115304.
(26) Koh, T. S.; Feng, Y. P.; Spector, H. N. Effects of Electric Field on Exciton Linewidth Broadening Due to Scattering by Free Carriers in Semiconducting Quantum-Well Structures. *IEEE J. Quantum Electron.* **1997**, *33*, 1774−1778.
(27) Jiang, H.; Singh, J. Linear Electro-Optic Effect Due to the Built-in Electric Field in InGaN/GaN Quantum Wells. *Appl. Phys. Lett.* **1999**, *75*, 1932−1934.
(28) Trautman, P.; Pakuła, K.; Bozek, R.; Baranowski, J. M. Light-Induced Narrowing of Excitonic Absorption Lines in GaN. *Appl. Phys. Lett.* **2003**, *83*, 3510−3512.
(29) Awasthi, K.; Iimori, T.; Ohta, N. Integral Method Analysis of Electroabsorption Spectra and Its Application to Quantum Dots of PbSe. *J. Phys. Chem. C* **2014**, *118*, 18170−18176.
(30) Miller, D. A. B.; Weiner, J. S.; Chemla, D. S. Electric-Field Dependence of Linear Optical Properties in Quantum Well Structures: Waveguide Electroabsorption and Sum Rules. *IEEE J. Quantum Electron.* **1986**, *22*, 1816−1830.
(31) Yasutomi, S.; Morita, T.; Imanishi, Y.; Kimura, S. A Molecular Photodiode System That Can Switch Photocurrent Direction. *Science* **2004**, *304*, 1944−1947.
(32) Gawęda, S.; Kowalik, R.; Kwolek, P.; Macyk, W.; Mech, J.; Oszajca, M.; Podborska, A.; Szaciłowski, K. Nanoscale Digital Devices Based on the Photoelectrochemical Photocurrent Switching Effect: Preparation, Properties and Applications. *Isr. J. Chem.* **2011**, *51*, 36−55.
(33) Sabeth, F.; Khaton, R.; Islam, M. S.; Iimori, T.; Ohta, N. Reversible Photocurrent Switching in Ionic and Superionic Conductors of Polycrystalline Silver Iodide. *J. Phys. Chem. C* **2018**, *122*, 26790−26796.
(34) Umeuchi, S.; Nishimura, Y.; Yamazaki, I.; Murakami, H.; Yamashita, M.; Ohta, N. Electric Field Effects on Absorption and Fluorescence Spectra of Pyrene Doped in a PMMA Polymer Film. *Thin Solid Films* **1997**, *311*, 239−245.
(35) Bublitz, G. U.; Boxer, S. G. STARK SPECTROSCOPY: Application in Chemistry, Biology, and Materials Science. *Annu. Rev. Phys. Chem.* **1997**, *48*, 213−242.
(36) Locknar, S. A.; Peteanu, L. A. Investigation of the Relationship between Dipolar Properties and Cis-Trans Configuration in Retinal Polyenes: A comparative Study Using Stark Spectroscopy and Semiempirical Calculations. *J. Phys. Chem. B* **1998**, *102*, 4240−4246.
(37) Stampor, W.; Kalinowski, J.; Di Marco, P. Electroabsorption Study of Vacuum-Deposited Films of Thionaphthenindole. *Chem. Phys.* **1989**, *134*, 385−393.
(38) Jalviste, E.; Ohta, N. Stark Absorption Spectroscopy of Indole and 3-Methylindole. *J. Chem. Phys.* **2004**, *121*, 4730−4739.
(39) Poglitsch, A.; Weber, D. Dynamic Disorder in Methylammoniumtrihalogenoplumbates (II) Observed by Millimeter-Wave Spectroscopy. *J. Chem. Phys.* **1987**, *87*, 6373−6378.
(40) Baikie, T.; Fang, Y.; Kadro, J. M.; Schreyer, M.; Wei, F.; Mhaisalkar, S. G.; Graetzel, M.; White, T. J. Synthesis and Crystal Chemistry of the Hybrid Perovskite $(CH_3NH_3)PbI_3$ for Solid-State Sensitized Solar Cell Applications. *J. Mater. Chem. A* **2013**, *1*, 5628−5641.
(41) Olthof, S.; Meerholz, K. Substrate-Dependent Electronic Structure and Film Formation of $MAPbI_3$Perovskites. *Sci. Rep.* **2017**, *7*, No. 40267.
(42) Climent-Pascual, E.; Hames, B. C.; Moreno-Ramirez, J. S.; Alvarez, A. L.; Juarez-Perez, E. J.; Mas-Marza, E.; Mora-Sero, I.; de Andres, A.; Coya, C. Influence of the Substrate on the Bulk Properties of Hybrid Lead Halide Perovskite Films. *J. Mater. Chem. A* **2016**, *4*, 18153−18163.
(43) Takahashi, S.; Uchida, S.; Jayaweera, P. V. V.; Kaneko, S.; Segawa, H. Impact of Compact TiO_2 Interface Modification on the Crystallinity of Perovskite Solar Cells. *Sci. Rep.* **2023**, *13*, No. 16068.
(44) Rudin, S.; Reinecke, T. L.; Segal, B. Temperature-Dependent Exciton Linewidths in Semiconductors. *Phys. Rev. B* **1990**, *42*, 11218−11231.

https://doi.org/10.1021/acs.jpcc.3c05603
J. Phys. Chem. C 2023, 127, 24383−24392